Adsorption, Coadsorption, and Reaction of Acetaldehyde and NO_2 on Na−Y,FAU: An In Situ FTIR Investigation

János Szanyi,* Ja Hun Kwak, Ryan A. Moline, and Charles H. F. Peden

Chemical Sciences Division, Pacific Northwest National Laboratory, P.O. Box 999, MS K8-93, Richland, Washington 99352

Received: May 5, 2004; In Final Form: August 3, 2004

The adsorption of acetaldehyde and its coadsorption and reaction with NO_2 were investigated on a Na−Y,FAU zeolite using in situ FTIR spectroscopy. Acetaldehyde adsorbs strongly over Na−Y and desorbs molecularly at around 400 K with very limited extent of condensation or polymerization. Reaction between CH_3CHO and NO_2 takes place in coadsorption experiments even at 300 K. In the initial step, acetaldehyde is oxidized to acetic acid accompanied by the formation of NO, which can be observed as N_2O_3 formed via a further reaction between NO and NO_2. The key intermediates in the overall NO_x reduction in this process are nitromethane and, possibly, nitrosomethane, which form in the next step. Their decomposition and further reaction with adsorbed NO_x species lead to the formation of HCN, HNCO, N_2O, CO_2, and organic nitrile species identified by their characteristic IR vibrational signatures. At 473 K, the reaction between adsorbed CH_3CHO and NO_2 is very fast. The results seem to suggest a mechanism in which N−N bond formation takes place among ionic nitrogen containing species (NO^+ and CN^- or NCO^-). No evidence has been found to suggest the participation of $NH_x^+NO_y^-$ type species in the N−N bond formation under the experimental conditions of this study, although their role in the overall N_2 formation process cannot be ruled out under realistic catalytic conditions.

Introduction

Traditional three-way catalysts are ineffective for the reduction of NO_x under oxygen rich engine operation; therefore, new technologies have been sought for exhaust emission control. Selective catalytic reduction with urea, selective NO_x ad/absorbers−reduction catalysts, and nonthermal plasma assisted NO_x reduction are some of the new methods being considered for emission control under lean engine operation.[1] In plasma assisted catalytic NO_x reduction,[1−11] a plasma source is placed between the engine outlet and the catalyst bed. The role of plasma is to generate reactive species that can be converted into nonharmful compounds over the catalyst. The primary effect of the plasma has been established as conversion of NO to NO_2 and partial oxidation of hydrocarbons. After these reactive species are formed in the plasma, their conversion can proceed on alkali and alkali earth ion exchanged Y,FAU zeolites.[4,5,7,9,10−12] Among the partially oxidized hydrocarbons formed in the nonthermal plasma, acetaldehyde has been shown to be particularly effective for the reduction of NO_2 to N_2.

Although there has been a number of investigations on the adsorption and reactions of acetaldehyde on oxide surfaces, IR spectroscopic studies on these processes are rare. In their FTIR spectroscopy study on the adsorption of acetaldehyde on silica surfaces, Hill et al.[13] have shown that oligomeric CH_3CHO could form from physisorbed CH_3CHO. They also report on the formation of acetic acid when oxygen is present in the system together with the adsorbed CH_3CHO. Oligomerization and aldol condensation of adsorbed CH_3CHO were also reported by Natal-Santiago et al.[14] on silica, and by Luo and Falconer[15] on titania, and very recently by Sachtler et al.[16] on Ba−Y zeolites.

In this paper, we report the results of an FTIR investigation on the adsorption of CH_3CHO, and the coadsorption and reaction of CH_3CHO and NO_2 over a Na−Y,FAU zeolite. The adsorption of CH_3CHO and its coadsorption with NO_2 were studied at 300 K. The reaction between NO_2 and CH_3CHO was investigated at both 300 K and 473 K.

Experimental Section

The experimental setup was identical to that we have described previously for the adsorption of NO_x on Na−Y[17] and Ba−Y.[18] Briefly, the IR cell was a six way metal cube equipped with CaF_2 windows attached to a pumping/gas handling manifold. The powder catalyst sample was pressed onto a fine-tungsten grid that, in turn, was mounted onto a copper sample holder assembly attached to a metal tube through metal/ceramic feed throughs. This setup allows operation in the $10^{-8} < P < 10^3$ Torr pressure range and the $110 < T < 1000$ K temperature range. The IR cell was mounted into the compartment of a Mattson Research Series FTIR spectrometer. The IR spectra were collected with 4 cm^{-1} resolution and recorded as the average of 64 scans. In all the experiments discussed here, the background was always collected with the clean sample in the IR beam, and this spectrum was subtracted from each IR spectrum taken after gas exposure. Therefore, the IR features observed represent only surface adsorbed species. Prior to each experiment, the sample was dehydrated at 673 K by annealing for 3 h. To ensure that no organic contaminants were left on the catalyst sample, two cycles of oxidation at 550 K for 30 min were also conducted.

The catalyst used throughout this study was a Na−Y,FAU obtained from Zeolyst International with a Si/Al ∼ 2.5 (CBV 100). NMR analysis showed that the material contained no

* Corresponding author. E-mail: janos.szanyi@pnl.gov. Tel: (509)-376-6466. Fax: (509)-376-5106.

10.1021/jp048064+ CCC: $27.50
Published on Web 10/13/2004

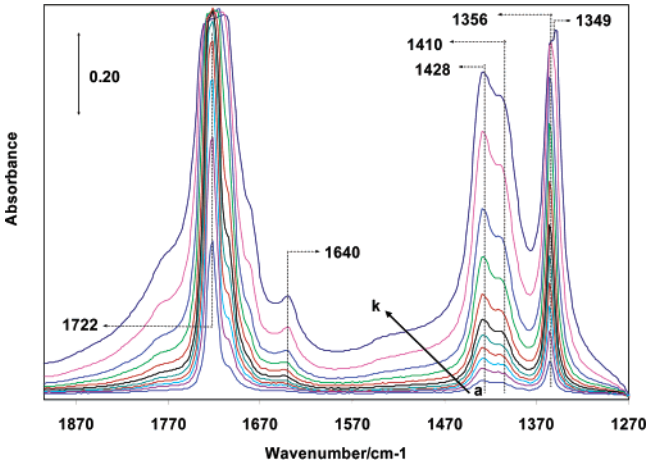

Figure 1. CH_3CHO adsorption on Na−Y,FAU at 300 K.

extraframework alumina. Acetaldehyde (Aldrich) was used as received after three cycles of freeze/pump/thaw cycles to remove volatile impurities. The NO_2 (Matheson) was cleaned by multiple freeze/pump/thaw cycles, while oxygen was used as received.

The acetaldehyde adsorption experiments were conducted as follows: acetaldehyde was introduced into the IR cell stepwise and after 3:00 min equilibration time, an IR spectrum was recorded after each adsorbate dose. In the acetaldehyde + NO_2 coadsorption experiments, after saturation of the zeolite with one of the adsorbates (acetaldehyde or NO_2), the cell was evacuated for 5−15 min to remove the excess (gas phase and weakly bound) adsorbate. The second adsorbate was then introduced either stepwise and the changes in the IR spectra were followed as a function of the amount of adsorbate dosed, or a given amount of the second adsorbate was introduced and IR spectra were recorded as a function of time.

The reaction studies were carried out at elevated temperatures, mostly at 473 K. The catalyst was first saturated with one of the adsorbates at room temperature, followed by the introduction of the second reactant. The sample temperature was then raised to 473 K for a given time period, followed by cooling back to room temperature. After the completion of a series of reaction experiments, the sample was annealed to increasingly higher temperatures for 1:00 min (at each temperature) and then cooled back to room temperature. All of the spectra reported here were recorded at room temperature.

Results and Discussion

1. CH_3CHO Adsorption. The adsorption of acetaldehyde (CH_3CHO) was investigated on a Na−Y,FAU zeolite both at room temperature and at 473 K. A series of IR spectra of room temperature adsorbed CH_3CHO with increasing dosages is shown in Figure 1 in the 1270−1900 cm^{-1} region. The spectra can be divided into three regions: (1) 1250−1450 cm^{-1}: deformation vibrations of CH_x groups; (2) 1680−1750 cm^{-1}: stretching vibration of the C═O double bond; (3) 2750−3050 cm^{-1}: C−H stretching vibrations of CH_x groups (not shown). At the lowest CH_3CHO coverage, the characteristic C═O stretching vibrational feature is centered at 1722 cm^{-1} with a small shoulder on its low frequency side. The position of the $\nu_{C=O}$ is red shifted by some 27 cm^{-1} in comparison to that of gas phase CH_3CHO. The small shoulder on the low frequency side of the main $\nu_{C=O}$ band probably arises from the heterogeneity of the adsorption sites inside the zeolite structure. The intensities of all the IR features increase with the increasing amount of CH_3CHO introduced into the cell. The intensity of the sharp $\nu_{C=O}$ band increases rapidly with the increasing amount of CH_3CHO introduced and then reaches its maximum. The intensity of the low frequency shoulder increases in the same manner. After the $\nu_{C=O}$ band reaches its maximum intensity, it broadens significantly as additional CH_3CHO is introduced into the cell. Its peak position also shifts toward lower wavenumbers. The broadening and the shift in the position of this band indicate multiple CH_3CHO adsorption onto the same adsorption centers, likely Na^+ cations. At high CH_3CHO doses, new features develop on both the low and high frequency sides of this band. As these new features appear, a shoulder (and then a distinct peak) develops at 1349 cm^{-1}; this indicates the presence of gas phase CH_3CHO. The position of the δ_{s,CH_3} band is much less sensitive to the adsorption of CH_3CHO than that of the $\nu_{C=O}$ band. The CH_3CHO adsorbs onto the cationic sites of the zeolite through the oxygen atom of the carbonyl group (partial negative charge on the carbonyl oxygen). Due to this interaction, there is some charge transfer from the carbonyl group to the cationic site that results in the weakening of the C═O double bond. The weakened C═O bond strength, in turn, results in the red shift of this vibrational feature. The interaction between the charge compensating cation and the O atom of the carbonyl group does not significantly affect the stretching and deformation vibrations of the CH_3 group of CH_3CHO. Therefore, only a small shift in the position of the δ_{s,CH_3} is expected upon adsorption. However, this small, approximately 6 cm^{-1} blue shift is sufficient to differentiate between adsorbed species and free, gas phase molecules. The shoulders developing on both the low and high frequency sides of the $\nu_{C=O}$ band at the highest dosages represent the $\nu_{C=O}$ of gas phase CH_3CHO. It is also interesting to note that a band develops at higher CH_3CHO doses at 1640 cm^{-1} that represents δ_{H_2O} vibrations. Water can form in the condensation reaction of CH_3CHO catalyzed by the solid material at higher CH_3CHO concentrations.

The interaction between CH_3CHO and the cationic sites of the zeolite is strong. Evacuation of the cell for an extended period of time at a 300 K sample temperature removes only the gas phase CH_3CHO. It does not significantly affect the adsorbed CH_3CHO. After 15 min evacuation, most of the adsorbed species on the cationic sites are still present. Even the adsorption complexes containing more than one CH_3CHO are fairly stable at 300 K, and there is hardly any change in the IR features of these species after the evacuation process. (The strong adsorption of CH_3CHO was also evidenced by a large jump (10−25 K) in sample temperature after each acetaldehyde dose.)

The adsorption of CH_3CHO was also carried out at a 473 K sample temperature (where the maximum catalytic activity is observed in the plasma assisted NO_x reduction over Na−Y). A series of IR spectra recorded at the 473 K sample temperature is displayed in Figure 2 in the 1300−1800 cm^{-1} region as a function of CH_3CHO pressure. For this series of FTIR data, a background spectrum with the sample in the IR beam was recorded at 473 K prior to CH_3CHO introduction. The IR signatures of adsorbed CH_3CHO can clearly be seen, even after the introduction of only a very small amount of CH_3CHO. Increasing the amount of CH_3CHO introduced into the cell results in large intensity gains of both the $\nu_{C=O}$ and δ_{s,CH_3} vibrational features. Under these conditions, no signatures of the adsorption complexes containing more than one CH_3CHO molecule are detected, as no significant broadening of the $\nu_{C=O}$ band is observed. These results confirm that CH_3CHO indeed adsorbs strongly onto the Na−Y,FAU catalyst. In a TPD

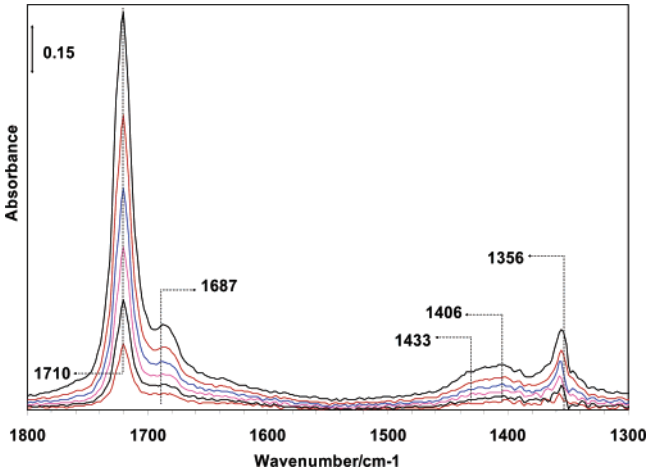

Figure 2. CH_3CHO adsorption on Na−Y,FAU at 473 K.

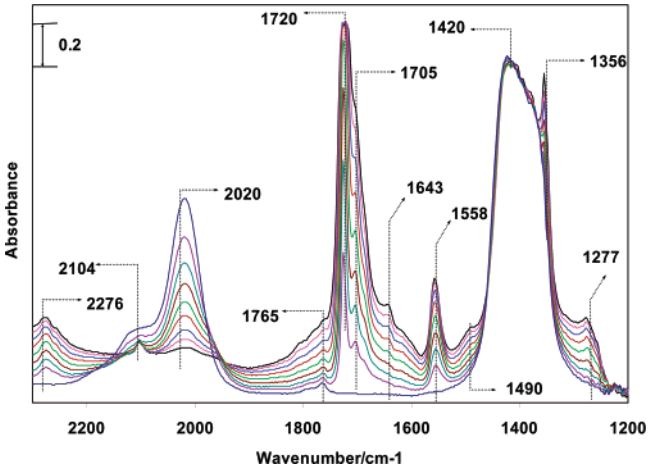

Figure 3. CH_3CHO adsorption on $(NO_2)_{ads}$−Na−Y,FAU at 300 K. The IR cell was evacuated for 5 min after the Na−Y,FAU sample was saturated with NO_2.

experiment of the acetaldehyde exposed sample, we observed one distinct desorption feature at ∼400 K (at 12 K/s heating rate). In the IR spectra collected during the high temperature (473 K) adsorption and the TPD experiments, no spectral features characteristic of crotonaldehyde or other condensed product can be seen. In their recent publication, Sachtler et al.[16] suggest that upon CH_3CHO adsorption on Ba−Y in the absence of water, aldol condensation can take place to produce crotonaldehyde, which may result in further condensation/polymerization, ultimately leading to catalyst deactivation by the thus formed carbonaceous deposits. This process, as they show, can be prevented by adding water to the feed gas mixture. In our experiments under the conditions applied (catalyst temperature and CH_3CHO pressure), no evidence for aldol condensation/polymerization was found.

2. Coadsorption of NO_2 and CH_3CHO at 300 K. Before presenting data on the coadsorption of NO_2 and CH_3CHO, we briefly review the results of our NO_2 adsorption studies on Na−Y.[17] On dehydrated Na−Y, upon disproportionation, NO_2 adsorbs as NO^+ and NO_3^- ion pairs. NO^+ occupies cationic positions of the Y,FAU structure, while NO_3^- adsorbs onto Na^+ ions. An IR absorption feature characteristic of the N−O vibration of NO^+ species is seen at 2020 cm^{-1}, while the IR signatures of adsorbed nitrates are observed in the 1370−1430 cm^{-1} spectral range. Upon exposure of Na−Y with a large amount of NO_2, the formation of NO^+NO_2 and/or $NO^+N_2O_4$ adducts is also seen (IR features at ∼2170 cm^{-1}). On Na−Y, these adducts, however, are held very weakly and can be removed by a brief room temperature evacuation. In fact, most of the adsorbed NO_2 can be removed from Na−Y at low temperatures. This was evidenced by the maximum NO_2 desorption rate at 345K in TPD experiments following NO_2 adsorption.[18] The formation of NO_2^- is also observed on partially dehydrated Na−Y, as an absorption feature at 1270 cm^{-1} appears upon NO_2 adsorption. The presence of one of the reactants on the catalyst may significantly influence the adsorption of the other. In the catalytic process we are interested in, both of these reactant molecules (NO_2 and CH_3CHO) are present; therefore, their coadsorption was of great interest.

A series of IR spectra recorded during the adsorption of CH_3CHO on a NO_2-saturated Na−Y,FAU is displayed in Figure 3 in the 1200−2300 cm^{-1} region. First, the catalyst was saturated with NO_2 at 300 K and then evacuated for 5 min. Subsequently, CH_3CHO was added to the system in increasing amounts. The IR features observed after the NO_2 saturation represent adsorbed NO_3^- (1370−1430 cm^{-1}) and NO^+ (2020 cm^{-1}) species, as we have discussed above.[17] After the first small amount of CH_3CHO is introduced, the features of adsorbed CH_3CHO and some new bands are observed in the IR spectrum. The $\nu_{C=O}$ band develops at 1724 cm^{-1}, practically at the same position as we have seen for the NO_2-free Na−Y. However, on the low frequency side of this band, a new feature can be seen at 1705 cm^{-1}, a distinct new peak appears at 1556 cm^{-1}, and a low intensity shoulder develops at around 1970 cm^{-1}. Increasing the amount of CH_3CHO introduced into the IR cell results in increases of the intensities of these bands. It also results in the development of some additional new features. With increasing amounts of CH_3CHO introduced, new bands appear at 1643, 1623, 1490, and 1277 cm^{-1}. Parallel to the development of these features is the intensity decrease of the 2020 cm^{-1} band. This latter feature completely disappears at the highest CH_3CHO dosages applied. Finally, a low intensity band develops at 2104 cm^{-1} and a broad feature also appears in the 2200−2300 cm^{-1} range as a result of CH_3CHO adsorption on the $(NO_2)_{ads}$−Na−Y zeolite.

The two most interesting observations in the adsorption of CH_3CHO on the NO_2-saturated Na−Y are the gradual disappearance of the 2020 cm^{-1} IR band associated with adsorbed NO^+ and the appearance of a $\nu_{C=O}$ band of adsorbed CH_3CHO at almost the same position as we have seen on the NO_2-free material. On fully NO_2-saturated Na−Y, the Na^+ ions are associated with NO_3^- ions and the negative charge of the zeolitic framework is compensated by NO^+ ions. If we assume that, upon NO_2 saturation, all of the Na^+ cations interact either with NO_3^- or NO_2^-, we might expect a marked effect on the strength of CH_3CHO adsorption that could be evidenced by a frequency shift in the $\nu_{C=O}$ band position. The observed lack of change in the $\nu_{C=O}$ of adsorbed CH_3CHO may then suggest that upon evacuation of the NO_2-saturated sample, a fraction of the adsorbed NO_2 ($NO^+NO_3^-$) has been removed, as we have shown previously,[18] opening up Na^+ sites for CH_3CHO adsorption. It is also possible that acetaldehyde can adsorb onto Na^+ sites associated with NO_3^- ions after having been replaced by NO^+ ions as charge compensation cations in the zeolite. However, the presence of the NO_3^- ion close to the Na^+ ion would be expected to influence significantly the adsorption characteristics of the Na^+ ions by modifying their chemical environment. The observed lack of change in the $\nu_{C=O}$ band position of adsorbed CH_3CHO does not support this argument. The intensity of the $\nu_{C=O}$ band is also very similar to what we have seen for CH_3CHO adsorbed on NO_2-free Na−Y, suggesting that the amount of adsorbed CH_3CHO is not influenced

significantly by the presence of preadsorbed NO_2 (assuming that the IR absorption cross sections of the $\nu_{C=O}$ vibration mode are the same for CH_3CHO adsorbed on free and NO_x^--adsorbed Na^+ sites). Thus, another possible explanation for these effects is that some of the adsorbed NO_2 ($NO^+NO_3^-$) react with the incoming CH_3CHO, thereby opening up adsorbate-free Na^+ sites for CH_3CHO adsorption.

The question now is what happens to the NO^+ species upon CH_3CHO adsorption that accounts for the disappearance of the 2020 cm^{-1} IR band? A couple of possibilities are (1) NO^+ reacts with incoming CH_3CHO molecules or (2) NO^+ is replaced by some species formed upon the introduction of CH_3CHO. Since CH_3CHO adsorbs onto Lewis acid sites, but not to the Lewis base sites that NO^+ is bonded to, we prefer the first possibility. The incoming CH_3CHO molecules can interact with both Na^+ and NO^+ ions. As noted above, CH_3CHO interacting with Na^+ ions gives rise to the observed carbonyl stretching vibration at practically the same position that we have seen for CH_3CHO on the clean Na−Y material (∼1724 cm^{-1}). On the other hand, when CH_3CHO interacts with $(NO_2)_{ads}$−Na−Y, a chemical reaction can be invoked to account for the appearance of new IR absorption features at 1556 and 1970 cm^{-1}, the disappearance of the 2020 cm^{-1} band, as well as the development of a new $\nu_{C=O}$ band at 1704 cm^{-1}.The suggestion that reaction takes place between adsorbed NO_x and the incoming CH_3CHO is also supported by the changes seen in the ν_{O-H} spectral region. As CH_3CHO interacts with $(NO_2)_{ads}$−Na−Y, the high frequency (HF) and low frequency (LF) O−H stretching vibrational features of bridging OH groups appear and increase in intensity with the increase in CH_3CHO introduced. Parallel to these are the development of new features at 1277, 1556, and 1970 cm^{-1}. The 1277 cm^{-1} band can be assigned to a NO_2^- species formed by the reaction between CH_3CHO and NO_3^-:

$$CH_3CHO + NO_3^- \rightarrow CH_3COOH + NO_2^- \quad \text{and/or } CH_3COO^- + H^+NO_2^- \quad (1)$$

This feature is the same one that we have observed upon the interaction of NO_2 and water on Na−Y.[18] Acidic protons formed via a reaction as depicted in eq 1 can now replace the NO^+ cations as charge compensating cations, which is evidenced by the development of IR features characteristic of acidic OH groups in Y,FAU structures. These NO^+ cations can then react with the thus formed acetate ions resulting in the formation of nitrosomethane and CO_2. The development of new IR features at 2104 and above 2200 cm^{-1} suggests that further reactions are occurring involving NO^+, as we will discuss later.

The assignments of the 1556 and 1970 cm^{-1} bands developed upon the coadsorption of NO_2 and CH_3CHO are not trivial. Isotopic labeling of the nitrogen atom in NO_2 (^{15}N for ^{14}N) results in a red shift of the 1556 cm^{-1} band to 1525 cm^{-1}, while substituting the ^{16}O atom with ^{18}O brings about an approximately 10 cm^{-1} red shift of this band. Similar shifts are seen for the 1970 cm^{-1} feature as well. These observations suggest that these bands represent N−O vibrational modes, and their spectral positions strongly support their assignments to adsorbed N_2O_3 species.[17,19,20] The fact that these species can readily be removed by a brief evacuation at room temperature also supports the assignment to weakly adsorbed N_2O_3. As we have shown previously,[17] N_2O_3 can adsorb onto Na−Y, though the adsorption is weak. We have to mention here that, though the intensity of the 1556 cm^{-1} band decreases dramatically upon room temperature evacuation, it does not disappear completely. This result suggests that the 1556 cm^{-1} band is, in fact, a composite one, and after evacuation a low intensity band centered at 1560 cm^{-1} is present. This small feature is the one that represents adsorbed nitromethane (NM), and not the high intensity, broad feature centered at ∼1550 cm^{-1} suggested recently by Orlando et al.[21] The formation of NM in the $CH_3CHO + NO_2$ reaction has been shown unambiguously in the IR study of Sachtler et al.[22] on a Ba(Na)−Y catalyst. The observed IR features representing adsorbed N_2O_3 (1556 and 1970 cm^{-1}) arise from the reaction between NO_2 (present as $NO^+NO_3^-$) and acetaldehyde, in which acetic acid and NO are formed. The thus produced NO can interact with NO_2 to form N_2O_3. We believe that both NO_2 and NO_3^- ions contribute to the initial oxidation step of acetaldehyde.

There are additional changes in the IR spectra upon the introduction of acetaldehyde onto the $(NO_2)_{ads}$−Na−Y. A band develops at 1640 cm^{-1} that represents adsorbed water formed in the reaction of the organic species with NO_x. As water is formed, the intensity of the HF zeolitic OH band increases. New low intensity features also develop at around 1620 and 1480 cm^{-1} that can be assigned to the ν_s and ν_{as} vibrations of adsorbed carboxylate ions. These species are formed upon the oxidation of acetaldehyde by NO_3^- ions and NO_2 (as we have discussed above).

The role of nitrate ions in the selective catalytic reduction of NO with propene has been investigated on Na−H−MOR[23] and alumina[24] catalysts. Surface nitrates were suggested to be active intermediates in the reaction with surface organic species. In fact, on Na−H−MOR this reaction was proposed as the rate determining step in the overall NO reduction with propene. Surface nitrates were found to be the oxygen carriers to the adsorbed organics and the primary source for N_2 formation.

There are two other vibrational features in the spectra that we need to assign: one sharp, low intensity feature at 2104 cm^{-1}, and another broad band (probably the composite of a number of individual vibrational features) in the 2220−2300 cm^{-1} region. As we will show in the following paragraphs, the 2104 cm^{-1} band can be assigned to HCN formed in the reaction between CH_3CHO and adsorbed NO_x species. The composite band originates primarily from N_2O and cyanates/isocyanates and nitriles. As we have mentioned above, nitroalkanes, most probably nitromethane, are formed during the reaction. Upon tautomerization, nitromethane can decompose and form HNCO:[25]

$$CH_3NO_2 \leftrightarrow CH_2{=}NO{-}OH \rightarrow HCNO + H_2O \rightarrow HNCO + H_2O \quad (2)$$

To gain further insight into the adsorption and reaction of CH_3CHO on the $(NO_2)_{ads}$−Na−Y catalyst, an experiment was carried out in which CH_3CHO was adsorbed onto a partially NO_2-saturated Na−Y sample. The series of IR spectra recorded in this experiment is shown in Figure 4 in the 1200−2300 cm^{-1} region. First, NO_2 was adsorbed onto a Na−Y sample in a quantity that is significantly smaller than that needed for saturation. Based on the comparison of integrated IR intensities of the NO^+ and NO_3^- bands, we conclude that the coverage is less than 50% of saturation. Upon the introduction of CH_3CHO, the band in the $\nu_{C=O}$ region resembles the one that was observed in the absence of adsorbed NO_2. This feature develops at 1725 cm^{-1} and it broadens as the amount of CH_3CHO introduced increases. The development of the adsorbed water IR feature at 1640 cm^{-1} can also be seen. The new features that we observed upon CH_3CHO adsorption on the NO_2-saturated Na−Y are significantly lower in intensity. The only feature we can clearly distinguish is the one at ∼1560 cm^{-1}, but its intensity is

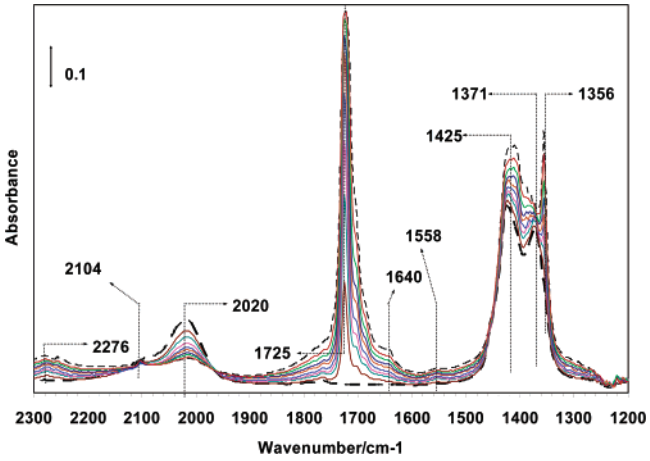

Figure 4. CH_3CHO adsorption on partially NO_2-covered [$\Theta_{NO_2} < 50\%$] Na−Y,FAU at 300 K. (The IR cell was evacuated at 300 K for 5 min following NO_2 adsorption.) [thick dashed spectrum: after NO_2 adsorption; thin dashed spectrum: after the highest CH_3CHO dose.]

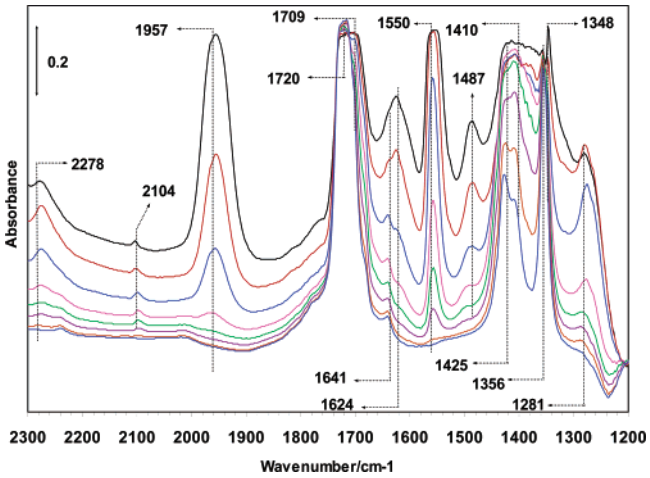

Figure 5. NO_2 adsorption on $(CH_3CHO)_{ads}$-Na−Y,FAU at 300 K.

extremely low throughout the CH_3CHO adsorption experiment. The intensity of the 2020 cm^{-1} band gradually decreases with the increasing amount of CH_3CHO added. On this partially NO_2-covered Na−Y, however, we cannot distinguish the band at around 1960 cm^{-1} that we have seen for the fully NO_2-saturated sample. These results suggest that CH_3CHO adsorbs onto acidic sites that are free of adsorbed NO_x species and also onto those sites that contain adsorbed NO_3^- species. The reaction between incoming CH_3CHO and adsorbed NO_x is slow in this case, due to the low concentration of one of the reactants, the adsorbed NO_x. Even under these conditions (low adsorbed NO_x concentration), the formation of HCN (2104 cm^{-1}), N_2O, HNCO, and nitriles (2220−2300 cm^{-1}) and water (1640 cm^{-1}) is apparent.

The interaction between CH_3CHO and NO_2 was also studied in a series of experiments in which acetaldehyde was adsorbed onto the Na−Y catalyst first (both at high and low coverages), and then NO_2 was gradually added into the system. In the first experiments the sample was saturated with CH_3CHO, and then the cell was evacuated for 5 min at 300 K. This was followed by the introduction of NO_2 into the cell, with increasing amounts. The series of IR spectra obtained in this experiment is displayed in Figure 5 in the 1200−2300 cm^{-1} region. After saturation with CH_3CHO, the broad $\nu_{C=O}$ band is seen at ~1720 cm^{-1} and $\delta(CH_3)$ vibrations are seen in the 1350−1450 cm^{-1} range. Upon the introduction of the first very small NO_2 dose, the appearance of only two bands at 1550 and 1280 cm^{-1} can be seen. There is also a significant intensity gain in the 1370−1420 cm^{-1} range due to the formation of NO_3^- species. With an increasing amount of NO_2 introduced, the intensities of these bands increase and new features develop at 1965−1957, 1624, and 1487 cm^{-1}. The 2020 cm^{-1} feature characteristic of adsorbed NO^+ on the CH_3CHO-free Na−Y,FAU is absent in the entire experiment. This suggests that all the sites available for NO_x adsorption have CH_3CHO associated with them, or the NO^+ species formed in the disproportionation of NO_2 on the surface of the solid catalyst react further in subsequent reactions. The intensities of the 1555 and 1280 cm^{-1} bands increase rapidly with increasing amounts of NO_2 introduced, and then they reach their maxima at the highest P_{NO_2}. The 1960, 1624, and 1487 cm^{-1} bands develop only after the third NO_2 aliquot is introduced. The intensities of these features increase rapidly upon further NO_2 introduction. The 1641 cm^{-1} band also gains intensity as the amount of NO_2 introduced increases. The intensity of the 1720 cm^{-1} band is decreased as the shoulder on the low frequency side develops. At the highest amount of NO_2 introduced, this shoulder (at ~1709 cm^{-1}) develops into a band as a result of the oxidation of CH_3CHO to acetic acid/acetate by the nitrate ions. The intensities of the 1556 and 1970 cm^{-1} features, representing adsorbed N_2O_3, are much higher here than we have seen in those experiments when NO_2 was adsorbed first and CH_3CHO was added second. This is expected, since a large amount of CH_3CHO is present on the sample and available for reaction with the incoming NO_2. As this reaction proceeds, N_2O_3 can form in relatively large quantities by the reaction between the in situ formed NO and the incoming NO_2 molecules and then, in turn, it can adsorb on the catalyst. Comparing the results of this experiment with those in which the "saturation" amount of NO_2 was adsorbed onto the Na−Y prior to CH_3CHO adsorption, it is evident that the intensities of the new features in the IR spectra (primarily the 1556 and 1970 cm^{-1} of adsorbed N_2O_3) are much higher in this case. This may suggest that the incoming NO_2 can oxidize the adsorbed CH_3CHO very effectively. Therefore, the large amount of NO formed in the reaction can easily form N_2O_3 with part of the incoming NO_2.

To gain further information about the interaction between NO_2 and CH_3CHO adsorbed onto Na−Y, we investigated the adsorption of NO_2 on a partially CH_3CHO-covered sample. First, we adsorbed a small amount of CH_3CHO onto the zeolite sample at 300 K. Based on the comparison of the integrated intensities of the $\nu_{C=O}$ band of the partially covered and fully saturated samples, the partially covered Na−Y was loaded with CH_3CHO to about 25% of its maximum capacity. Then, small aliquots of NO_2 were introduced into the IR cell and the spectral changes were followed as a function of the amount of NO_2 introduced. The series of IR spectra obtained in this experiment is shown in Figure 6 in the 1200−2300 cm^{-1} region. After the introduction of NO_2, a very broad band appears in the 1950−2150 cm^{-1} spectral region. This feature is the composite of several bands. Part of this band (at >2000 cm^{-1}) represents NO^+ species adsorbed to base sites, while the lower frequency portion of this band represents N_2O_3 as we have discussed above. Concomitantly, the intensity of the $\nu_{C=O}$ band at 1724 cm^{-1} decreases and the shoulder on its low frequency side intensifies. New bands at 1556 and 1279 cm^{-1} start developing as well, just as we have seen in the case of NO_2 adsorption on the fully CH_3CHO-saturated Na−Y. With increasing amounts of NO_2 introduced, the intensities of the 2020, 1967, 1556, and 1279 cm^{-1} bands all increase, while that of the 1724 cm^{-1} feature decreases. The new band at 1705 cm^{-1} gradually gains intensity as the 1724 cm^{-1} band loses its intensity. The adsorbed species

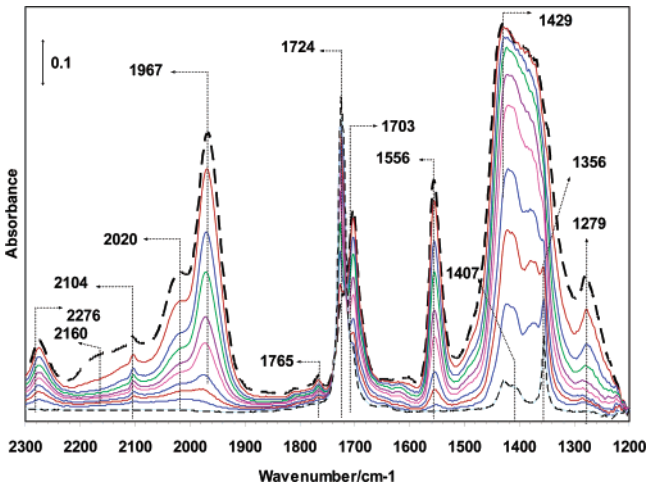

Figure 6. NO_2 adsorption on partially CH_3CHO-covered [Θ_{CH_3CHO} < 30%] Na−Y,FAU at 300 K. (The IR cell was evacuated at 300 K for 5 min following CH_3CHO adsorption.) [thin dashed spectrum: after CH_3CHO adsorption; thick dashed spectrum: at maximum NO_2 dose.]

represented by the 1724 cm^{-1} band is converted into another species with an absorption band centered at 1703 cm^{-1}, as the amount of NO_2 adsorbed increases as evidenced by the isosbestic point observed at 1712 cm^{-1}.

Comparison of the IR spectra recorded upon the adsorption of NO_2 on the fully and partially CH_3CHO-covered Na−Y allows us to draw some conclusions on the coadsorption/reaction of CH_3CHO and NO_2 at room temperature. On the partially CH_3CHO-saturated sample, NO^+ can adsorb onto centers that are free of adsorbed CH_3CHO, while no NO^+ species are seen on the fully acetaldehyde covered sample. As NO_2 adsorbs onto the catalyst, the intensity of the 1724 cm^{-1} band of adsorbed CH_3CHO decreases, and simultaneously a new band develops at 1705 cm^{-1}. The interconversion of the 1724 cm^{-1} band into the 1705 cm^{-1} feature can clearly be seen in the case of NO_2 adsorption on the partially CH_3CH-covered Na−Y. This phenomenon is more difficult to observe on the fully CH_3CHO-saturated sample, though we can observe a small decrease in the intensity of the 1724 cm^{-1} band and the development of a new feature as a shoulder at 1705 cm^{-1}. One might argue that the interconversion of these two $\nu_{C=O}$ vibrational features is the consequence of coadsorption of CH_3CHO with some ionic NO_x species, most probably with NO^+. Using the same argument, it could be concluded that the 1970 cm^{-1} band corresponds to a NO^+ species that is coadsorbed with acetaldehyde. These arguments, however, are not valid. Evacuation of the sample after NO_2 adsorption on $(CH_3CHO)_{ads}$-Na−Y at room temperature completely eliminates the 1970 cm^{-1} (and also the 1556 cm^{-1}) band, but there is no change in the intensity of the 1705 cm^{-1} feature.

To follow the evolution of the IR features discussed above as a function of time, an experiment was conducted in which given amounts of CH_3CHO and NO_2 were adsorbed onto a Na−Y catalyst at 300 K, and IR spectra were recorded periodically during a 60 min time interval. The integrated IR intensities of selected vibrational features as a function of time-on-stream are plotted in Figure 7. In this particular experiment the Na−Y catalyst was first exposed to NO_2 and then, without pumping the excess NO_2 out, CH_3CHO was introduced. This plot clearly shows that the features at 1970 and 1560 cm^{-1} follow exactly the same trend. At the beginning of the reaction, their intensities increase sharply, and they gradually decrease after reaching their maxima. This behavior can be explained by the large amount of NO formed in the first step of the

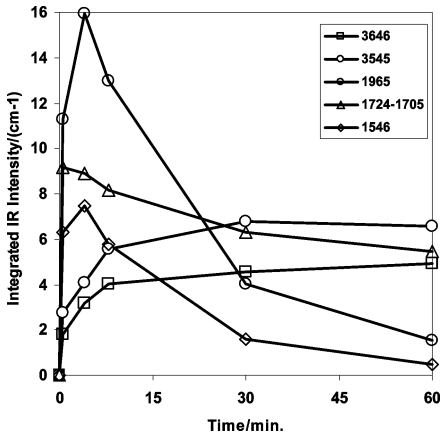

Figure 7. The time dependence of the integrated intensities of selected IR absorption features observed in the CH_3CHO + NO_2 reaction over Na−Y at 300 K.

reaction, which then can react with NO_2 to form adsorbed N_2O_3. As the reaction proceeds, the concentration of NO_2 available for the formation of N_2O_3 with the thus formed NO drops. Therefore, the NO + NO_2 ↔ N_2O_3 equilibrium is shifted to the left. Meanwhile, the intensity of the ν_{CO} vibrations (sum of the intensities of the 1724 and 1705 cm^{-1} features) decreases gradually with reaction time. After 1 min time-on-stream, most of the intensity of this feature comes from the 1705 cm^{-1} band due to the setup of this particular experiment (large amount of initial NO_2 present in the system). This implies that the oxidation of CH_3CHO, the initial reaction in the overall reaction mechanism, is facile even at 300 K over this catalyst, and the thus formed CH_3COOH is gradually converted to other products by the adsorbed NO_x species. The intensities of both HF and LF zeolitic OH vibrations (>3500 cm^{-1}) increase fast at the beginning of the reaction and then remain almost unchanged at longer reaction times.

3. Reaction between NO_2 and CH_3CHO at 473 K. The primary goal of this investigation was to gain some insight into the interaction between NO_2 and CH_3CHO on Na−Y,FAU that might bring us closer to understanding the mechanisms of reactions that take place over these catalysts. We have shown that both reactants adsorb strongly onto the zeolite catalyst and chemical reactions can take place between the two reactants even at room temperature. These low temperature coadsorption experiments are very useful in identifying intermediates that probably could not be seen at higher reaction temperature due to their high reactivities. In the next step, we investigated the reaction between the two reactants at a temperature where maximum catalytic activities have been observed in the non-thermal plasma assisted catalytic NO_x reduction under realistic operational conditions.[10,11] In a typical experiment, we first saturated the sample with one of the reactants at 300 K, and then introduced a certain amount of the other reactant. The sample was then heated at 473 K for a given period of time and finally cooled back down to room temperature. After each step, an IR spectrum was recorded at room temperature. We followed the changes in the intensities of the earlier assigned IR features, and the new ones that developed as a result of the reaction between CH_3CHO and NO_x at elevated temperatures. Upon completion of a reaction run (usually after 7 or 15 min total time-on-stream), we evacuated the cell for 5 min and took an IR spectrum to monitor the adsorbed species that remained strongly held on the catalyst at room temperature.

A series of IR spectra recorded in the reaction experiment as a function of reaction time is displayed in Figure 8 in the 1200−

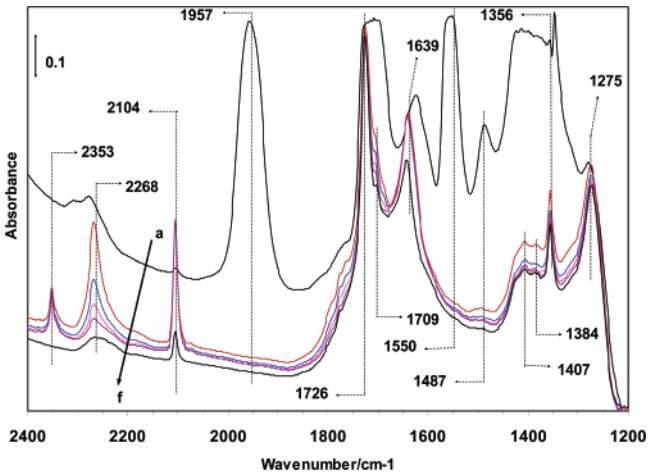

Figure 8. Reaction between NO_2 and CH_3CHO over Na−Y,FAU at 473 K. Spectrum **a**: prior to heating the sample to 473 K; **b**, **c**, **d**, and **e**: after 1, 3, 7, and 15 min reaction at 473 K; **f**: after 5 min evacuation at 300 K following spectrum **e**.

2400 cm^{-1} spectral region. Spectrum **a** is identical to spectrum **g** in Figure 5 and represents a system that contains only adsorbed CH_3CHO (saturated) and 0.1 Torr NO_2. The most dramatic changes in the IR spectrum occur after heating the sample at 473 K for 1:00 min. The IR features that developed upon NO_2 introduction onto the CH_3CHO-saturated sample (1957, 1624, 1556, and 1487 cm^{-1}) almost completely disappeared during this brief time period. The broad band between 1370 and 1430 cm^{-1}, which we assigned to NO_3^- species, lost most of its intensity as well, while the feature at 1275 cm^{-1} remained practically unchanged. There was also a very significant drop in the intensity of the broad band at 1720−1705 cm^{-1}. At the same time, new IR features developed at 2104, 2270, and 2353 cm^{-1}. The intensity of the 2104 cm^{-1} band increased sharply during the first minute of reaction. Subsequent heating for 2 min at 473 K resulted only in a small intensity increase of this band. At longer reaction times, the intensity of this feature remained almost constant, and dropped slightly after 15 min time-on-stream. The intensity of the 2353 cm^{-1} band increased significantly in the first 3 min of time-on-stream, and then it remained constant. The intensity of the broad band in the 2200−2300 cm^{-1} region increased dramatically after 1 min heating of the sample at 473 K, and then it gradually decreased with time-on-stream.

Upon completion of the 15 min reaction run, the cell was evacuated at room temperature for 5 min, and then an IR spectrum was acquired. The brief evacuation completely removed the adsorbed species responsible for the 2353 cm^{-1} band (spectrum **f**). The position of this band is very close to that of gas phase CO_2 and represents the ν_3 asymmetric stretching vibration of weakly adsorbed CO_2. The adsorption of CO_2 has been extensively studied on zeolite materials, primarily to gain insight into the basicity of alkali ion exchanged materials.[26,27] Data are available even for the CO_2/Na−X,FAU[28] and CO_2/Na−Y,FAU[29] systems. In zeolites, CO_2 physically adsorbs onto the cationic sites; in some cases, it can form carbonates with basic O^- sites of the zeolite framework. The weak adsorption bond between CO_2 and Lewis acid sites results in a small blue shift in the ν_3 asymmetric C═O vibration. The frequency shift is characteristic of the cation−dipole interaction. The weak bond between adsorbed CO_2 and Na^+ is also evidenced by the easy removal of CO_2 produced, manifested by the disappearance of the 2353 cm^{-1} band upon a brief evacuation at room temperature. To ensure that the 2353 cm^{-1} band represents weakly adsorbed CO_2 on the Na^+ sites of the catalyst, the adsorption of CO_2 was investigated at 300 K on the Na−Y,FAU zeolite. The only absorption feature at low P_{CO_2} was one at 2354 cm^{-1} (spectra are not shown for brevity). The bands at 2104 and 2270 cm^{-1} represent adsorbates more strongly bonded to the catalyst than CO_2. The intensity of the 2104 cm^{-1} band drops significantly upon the 5 min evacuation, but it still has significant intensity after this procedure. We assign the 2104 cm^{-1} band to the ν_{CN} vibration of molecularly adsorbed HCN, and the broad band between 2200 and 2300 cm^{-1} to a mixture of features due to adsorbed N_2O, isocyanate, and possibly organonitrile.

The formation of HCN, CH_3CN, and N_2O has been reported on a Ag/Al_2O_3 catalyst in the NO + O_2 + CH_3CH_2OH and NO + O_2 + CH_3CHO reactions.[30] The HCN was suggested to form through the direct reduction of NO by ethanol or acetaldehyde. The presence of HCN in the NTP-assisted lean NO_x reduction process has been observed by Schmieg et al.[3] and Tonkyn et al.[9] The position of the 2104 cm^{-1} band we observe when CH_3CHO reacts with NO_2 is very close to those reported in the literature for adsorbed HCN. For example, the ν_{CN} vibration of adsorbed HCN was observed at 2095 cm^{-1} on δ-alumina[31] and at 2100 cm^{-1} on silica.[32] In a recent study of the adsorption of HCN on silica and titania supported Rh catalysts,[33] the ν_{CN} vibration of adsorbed HCN was reported at 2096 and 2105 cm^{-1} for the titania and silica supports, respectively. Therefore, we attribute the 2104 cm^{-1} band to adsorbed HCN formed in the reaction of NO_x with acetaldehyde. The stability of this adsorbed species on the surface is higher than that of adsorbed CO_2. (The assignment of the 2104 cm^{-1} IR feature to weakly adsorbed HCN was confirmed in our subsequent studies on the interactions of HCN and NO_x and both Na−Y and Ba−Y.[34])

The broad band between 2200 and 2300 cm^{-1} probably represents more than one adsorbed species. The IR signature of adsorbed N_2O is around 2250 cm^{-1}. We suggest that the intense band that develops at 2260−2270 cm^{-1} as the NO_2 + CH_3CHO reaction proceeds arises from adsorbed N_2O and/or HNCO. The adsorption of these compounds onto the Na−Y,FAU catalyst is weak, as evidenced by the ready removal of the 2260−2270 cm^{-1} IR feature after the brief evacuation at 300 K. The remaining features in this spectral range probably belong to adsorbed isocyanate and nitrile molecules.

The large drop in the C═O stretching vibrational band of adsorbed CH_3CHO/CH_3COOH after a 1 min reaction at 473 K is remarkable. The very broad band we attributed to multiple CH_3CHO adsorption on cationic sites is reduced into a sharp band centered at 1726 cm^{-1}. Note also that upon the interaction of NO_x with CH_3CHO, an intense band of adsorbed water is seen at 1640 cm^{-1}. After the 5 min evacuation, the intensity of this band decreases somewhat, but there is still a large amount of adsorbed water present.

Following the evacuation of the system for 5 min at 300 K, we introduced another aliquot of NO_2 into the cell and carried out the reaction for another 15 min The P_{NO_2} in the cell was 0.3 Torr at the beginning of the reaction. The IR spectra recorded at room temperature after each heating step are displayed in Figure 9 in the 1200−2400 cm^{-1} region. After the introduction of NO_2 into the cell, the same N−O vibrational features at 1963, 1556, and 1350−1450 cm^{-1} develop as we have seen prior to the first reaction series. Note the large increase in the intensity of the 1703 cm^{-1} band that we have attributed to the C═O stretching vibration of adsorbed CH_3COOH formed by the oxidation of CH_3CHO. Upon the first 1:00 min time-on-stream at 473 K, the large N−O features at 1963 and 1556 cm^{-1} almost

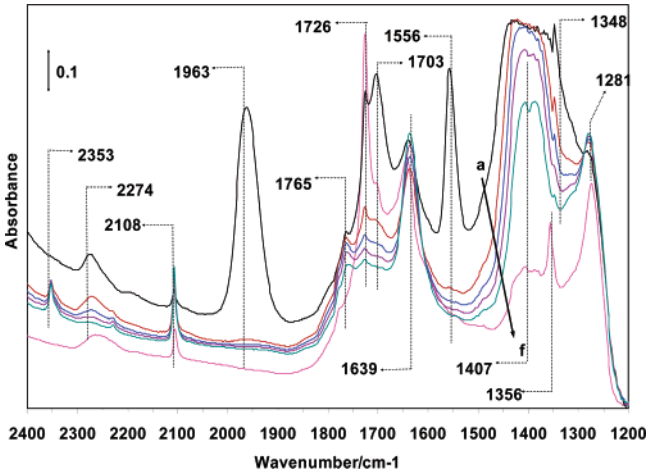

Figure 9. Reaction between NO_2 and CH_3CHO over Na−Y,FAU at 473 K. After spectrum **e** in Figure 9, 0.3 Torr of NO_2 was added to the system and the same series of experiments was run as described for Figure 9.

completely disappear, and the intensity of the 1703 cm^{-1} band decreases dramatically as well. Concomitant to these spectral changes are the appearance and growth of the features at 2353 and 2104 cm^{-1}due to adsorbed CO_2 and HCN, respectively. The spectral changes during the next 14 min reaction are much less dramatic. The $\nu_{C=O}$ band of adsorbed CH_3COOH decreases further, while the intensities of the 2353 and 2104 cm^{-1} bands increase gradually. The intensity of the 1640 cm^{-1} band (adsorbed water) also increases throughout the reaction. At the conclusion of the reaction there are still some IR signatures of adsorbed CH_3CHO/CH_3COOH, and the intensities of features in the 1200−1450 cm^{-1} region are higher than they were after the first reaction series. The integrated intensities of the 2104 and 2353 cm^{-1} bands were approximately 60% of those observed after the first reaction series. This is probably due to the fact that the amount of CH_3CHO present on the catalyst was significantly reduced during the first reaction series, thus decreasing the reaction probability between adsorbed organic and NO_x species.

4. Mechanistic Implications. The mechanistic picture that arises from the results of the adsorption and reaction experiments discussed above is as follows. There is a very strong interaction between CH_3CHO and adsorbed ionic NO_x species. The initial step of the reaction is the oxidation of acetaldehyde to acetic acid and acetate ions by NO_2 and NO_3^- ions. This process is substantiated by the appearances of IR bands characteristic of NO_2^- (1277 cm^{-1}), adsorbed acetic acid (1704 cm^{-1}), acetate ions (1623 and 1480 cm^{-1}), water (1640 cm^{-1}), and zeolitic OH (3646 and 3550 cm^{-1}) vibrations. At the same time, the formation of N_2O_3 is seen as evidenced by the development and increase of band intensities at 1556 and 1970 cm^{-1}. The intensities of these two bands always follow each other very closely (e.g., see Figure 7), demonstrating that they arise from the same adsorbed species. The development of the IR signatures of CO_2 (2353 cm^{-1}), HCN (2104 cm^{-1}), N_2O (2260 cm^{-1}) and organic nitriles, and cyanates/isocyanates (>2200 cm^{-1}) show that the acetate, formed in the initial reaction, further reacts with adsorbed NO_x species (most probably with NO^+ (2020 cm^{-1})). This initially forms nitromethane and, possibly, nitrosomethane, followed by their decomposition/reaction products. Our results suggest that these organic N-containing compounds (nitromethane and nitrosomethane) are, in fact, key intermediates in the NO_x reduction process with NO_2 over Na−Y. The decomposition of nitrosomethane (CH_3NO) favors the formation of HCN, while HNCO forms from CH_3NO_2. We need to emphasize here that the mechanism we propose does not necessarily need to involve nitrosomethane as a key intermediate. HCN, and subsequently CN^-, can form in the thermal decomposition of nitromethane and in the nitromethane + NO_2 reaction over both Na−Y and Ba−Y catalysts.[34] Our inability to observe any ammonia or NH_x-containing intermediates/products makes us believe that the mechanism of this process is different from other NO_x reduction processes, where nitrogen formation was explained by the formation and subsequent decomposition of NH_4NO_2.[35] This difference may originate from the principally different catalyst material used here (Na−Y), in contrast to the transition metal ion (Cu, Fe, Co, etc.) containing zeolites used in other studies for NO_x reduction. We believe that in our system the formation of the N−N bond takes place by the interaction of ionic N-containing species such as CN^-, NCO^-, and NO^+. This mechanism will be discussed in detail for both Na−Y and Ba−Y zeolites in our subsequent publication.[34] In a recent IR study by Sachtler et al.,[22] the participation of NH_4NO_2 in the N−N bond formation was suggested even over the basic Ba(Na)−Y,FAU zeolite catalysts. Most of the intermediates they identified are present in the Na−Y catalyst discussed here, and they are also in Ba−Y we will discuss elsewhere.[34] In both studies, the key intermediate seems to be the organic nitro compound that can itself decompose or react further with NO_x to form the reactive species that are precursors for the N−N bond formation. In our studies, we believe that these ionic precursors are CN^- and NCO^-; however, we cannot rule out an alternate route for the N−N bond formation, that is, the decomposition of NH_4NO_2. The relative importance of these parallel paths in the N−N bond formation may strongly depend on the conditions under which the particular study is conducted.

Conclusions

The adsorption of CH_3CHO is strong on Na−Y,FAU at 300 K. At low acetaldehyde partial pressures, the adsorption complex contains one acetaldehyde per Na^+. At higher CH_3CHO pressures, more than one CH_3CHO can adsorb onto each Na^+ adsorption center. The formation of adsorbed water may suggest that aldol condensation and/or oligomerization of CH_3CHO can take place on the Na−Y,FAU catalyst, although only to a limited extent.

Acetaldehyde reacts readily with NO_2 on Na−Y,FAU, even at 300 K, while the reaction between these two species is very fast at 473 K. The formation of CO_2, HCN, N_2O, NCO, organonitrile, and H_2O was observed in the reaction. Both NO^+ and NO_3^- seem to participate in these reactions. The IR band assigned to adsorbed NO^+ completely disappears, while the intensities of the bands characteristic of adsorbed NO_3^- decrease significantly during the course of the reaction. Parallel to the disappearance of the nitrate features is the development of a band representing adsorbed NO_2^-. This observation suggests that adsorbed NO_3^- plays a significant role in the oxidation of organic compounds over this catalyst.

The results presented in this study allow us to conclude that the initial step of the NO_2 + CH_3CHO reaction is the oxidation of the aldehyde to the corresponding carboxylic acid. Further reactions of the acetate ions with adsorbed NO_x species results in the formation of the key intermediates, nitromethane and possibly nitrosomethane. (Clear spectroscopic evidence for the formation of nitromethane is shown, while the participation of nitrosomethane in the reaction mechanism was inferred from the observed products of the overall reaction.) Then, in turn, these intermediates can undergo decomposition, as well as

further reactions with NO_2 ($NO^+NO_3^-$), ultimately producing the ionic species that lead to the formation of N−N bonds (either N_2 or N_2O). Our data do not seem to support a mechanism that would involve the formation of NH_x-containing reaction intermediates for the N−N bond formation. However, under significantly different reaction conditions, their participation in the overall N_2 formation process cannot be ruled out.

Acknowledgment. The authors gratefully acknowledge the U.S. Department of Energy (DOE), Office of Energy Efficiency and Renewable Energy, FreedomCAR and Vehicle Technologies for support of this program. The work was performed as part of a CRADA with the USCAR Low Emissions Technologies Research and Development Partnership (LEP), Pacific Northwest National Laboratory (PNNL), and DOE/OFCVT. The research described in this paper was performed at the Environmental Molecular Sciences Laboratory, a national scientific user facility sponsored by the DOE Office of Biological and Environmental Research and located at the Pacific Northwest National Laboratory (PNNL). PNNL is operated for the U.S. DOE by Battelle Memorial Institute under Contract No. DE-AC0676RLO1831.

References and Notes

(1) Johnson, T. V. *SAE* SP-1581 23−39, 2001.
(2) Hammer, T.; Kishimoto, T.; Krutzsch, B.; Andorf, R.; Plog, C. *SAE* SP-1639 81−86, 2001.
(3) Schmieg, S.; Cho, B.; Oh, S. H. *SAE* SP-1639 69−80, 2001.
(4) Panov, A. G.; Tonkyn, R. G.; Balmer, M. L.; Peden, C. H. F.; Malkin, A.; Hoard, J. W. *SAE* SP-1639 43−48, 2001.
(5) Hoard, J. W.; Panov, A. G. *SAE* SP-1639 29−42, 2001.
(6) Fisher, G. B.; DiMaggio, C. L.; Yezerets, A.; Kung, M. C.; Kung, H. H.; Baskaran, S.; Frye, J. G.; Smith, M. R.; Herling, D. R.; LeBarge, W. J.; Kupe, J. *SAE* Sp-1566 79−87, 2000.
(7) Panov, A. G.; Tonkyn, R. G.; Yoon, S.; Kolwaite, A.; Barlow, S.; Balmer, M. L. *SAE* SP-1566 73−77, 2000.
(8) Lampert, J. K. *SAE* SP-1566 67−72, 2000.
(9) Tonkyn, R. G.; Yoon, S.; Barlow, S. E.; Panov, A. G.; Kolwaite, A.; Balmer, M. L. *SAE* SP-1566 35−41, 2000.
(10) Kwak, J. H.; Szanyi, J.; Peden, C. H. F. *J. Catal.* **2003**, *220*, 291.
(11) Kwak, J. H.; Szanyi, J.; Peden, C. H. F. *Catal. Today* **2004**, *89* (1−2), 135.
(12) Schmieg, S. J.; Cho, B. K.; Oh, S. H. *Applied Catal. B: Environmental* **2004**, *49*, 113.
(13) Hill, W.; Miessner, H.; Ohlman, G. *J. Chem. Soc., Faraday Trans. 1* **1989**, *85* (3), 691.
(14) Natal-Santiago, M. A.; Hill, J. M.; Dumesic, J. A. *J. Mol. Catal. A: Chemical* **1999**, *140*, 199.
(15) Luo, S.; Falconer, J. L. *J. Catal.* **1999**, *185*, 393.
(16) Wen, B.; Yeom, Y. H.; Weitz, E.; Sachtler, W. M. H. *Appl. Catal. B: Environmental* **2004**, *48*, 125.
(17) Szanyi, J.; Kwak, J. H.; Moline, R. A.; Peden, C. H. F. *PCCP* **2003**, *5* (18), 4045.
(18) Szanyi, J.; Kwak, J. H.; Peden, C. H. F. *J. Phys. Chem, B* **2004**, *108*, 3746.
(19) Chao, C.-C.; Lunsford, J. H. *J. Am. Chem. Soc.* **1971**, *93* (25), 6794.
(20) Chao, C.-C.; Lunsford, J. H. *J. Am. Chem. Soc*. **1971**, *93* (1), 71.
(21) Orlando, T. M.; Alexandrov, A.; Lebsack, A.; Herring, J.; Hoard, J. W. *Catal. Today* **2004**, *89* (1−2), 151.
(22) Yeom, Y. H.; Wen, B.; Sachtler, W. M. H.; Weitz, E. *J. Phys. Chem. B* **2004**, *108*, 5386.
(23) Satsuma, A.; Enjoji, T.; Shimizu, K.; Sato, K.; Yoshida, H.; Hattori, T. *J. Chem. Soc. Faraday Trans.* **1998**, *94* (2), 301−307.
(24) Shimizu, K.; Kawabata, H.; Satsuma, A.; Hattori, T. *J. Phys. Chem. B* **1999**, *103*, 5240−5245.
(25) (a) Cant, N. W.; Cowan, A. D.; Doughty, A.; Haynes, B. S.; Nelson, D. F. *Catal. Lett.* **1997**, *46* (3,4), 207. (b) Cowan, A. W.; Cant, N. W.; Haynes, B. S.; Nelson, P. F. *J. Catal.* **1998**, *176*, 329.
(26) Forster, H.; Schuman, M. *J. Chem. Soc., Faraday Trans. 1* **1989**, *85* (5), 1149.
(27) Bonelli, B.; Civalleri, B.; Fubini, B.; Ugliengo, P.; Otero Orean, C.; Garrone, E. *J. Phys. Chem. B* **2000**, *104*, 10978.
(28) Lavalley, J. C. *Catal. Today* **1996**, *27*, 377.
(29) Martra, G.; Ocule, R.; Marchese, L.; Centi, G.; Coluccia, S. *Catalysis Today* **2002**, *73*, 83−93.
(30) Miyadera, T. *Appl. Catal. B: Environmental* **1997**, *13*, 157.
(31) Krietenbrink, H.; Knotzinger, H. *Z. Phys. Chem.* **1976**, *102*, 43−56.
(32) Morrow, B. A.; Cody, I. A. *J. Chem. Soc., Faraday 1* **1975**, *71*, 1021.
(33) Rasko, J.; Bansagi, T.; Solymosi, F. *Phys. Chem. Chem. Phys.* **2002**, *4*, 3509−3513.
(34) Szanyi, J.; Kwak, J. H.; Peden, C. H. F. *in preparation*.
(35) Sun, Q.; Gao, Z. X.; Chen, H. Y.; Sachtler, W. M. H. *J. Catal.* **2001**, *201*, 89.